Unusual features in trap emission characteristics of heavily damaged silicon induced by MeV ion implantation

P K Giri†§ and Y N Mohapatra‡

† Materials Science Division, Indira Gandhi Centre for Atomic Research,
Kalpakkam-603102, India
‡ Department of Physics, Indian Institute of Technology, Kanpur 208016, India

E-mail: `pkgiri@igcar.ernet.in`

Abstract. We have investigated the electrical characteristics of defects in heavily damaged silicon induced by MeV ion implantation at high doses, by extending the scope of depletion layer capacitance transient techniques. The heavily damaged layer is embedded in the depletion layer of a Schottky diode and high-frequency capacitance measurements are carried out to evaluate charge relaxation kinetics of defects specific to high-dose implantation. Deep-level transient spectroscopy of as-implanted silicon shows presence of the divacancy trap (V_2) and relatively high concentration of a damage-related trap (D1) with unusual spectral lineshape. Thermally stimulated capacitance spectra show large capacitance step even without application of a trap-filling pulse. Constant-capacitance time-analysed transient spectroscopy studies of the D1 peak reveal that the skewed peakshape is due to premature termination of the transient signal during trap emission. Strong temperature dependence of spectral lineshape, ranging from broad to narrow peak (stronger than that expected from exponential transient), and trap occupancy points to a dynamic interdependence of trap occupancy and quasi-Fermi level. Unusual features in spectral lineshape are simulated by introducing a time-dependent capture term into the rate equations for trapping dynamics for a single trap level and provide strong support for our model on the dynamic interdependence of quasi-Fermi level and trap occupancy. The defect parameter is found to be sensitive to implantation dose and low-temperature annealing. The D1 trap is ascribed to small self-interstitial clusters.

1. Introduction

Ion implantation is one of the key processing tools in silicon integrated circuit technology. In view of emerging applications of MeV ions in silicon processing, there has been an intensive effort to study defects and defect processes in high-dose MeV heavy-ion implanted silicon [1, 2]. While the defects induced by light-ion irradiations at low doses are well characterized in the literature using conventional electrical characterization tools [3, 4], defects resulting from high-dose implantation are much less understood. It is probable that differences in defect structures and their electrical behaviour in the case of high-dose implantation is due to migration of point defects and interaction among such defects, which may result in more a complex defect structure [5, 6]. Although a variety of structural tools have been used to study defects due to high-dose implantation and subsequent annealing, electrical studies in the high-dose

regime have been meagre, principally due to limitations of the techniques used and interpretational difficulties [7, 8]. The presence of a high density of traps embedded in a disordered environment make it difficult to use standard capacitance-based depletion layer spectroscopic techniques. Deep-level transient spectroscopy (DLTS) [9] has been extensively used in studies of defects in semiconductors, despite its inherent limitations. While conventional DLTS analysis rest upon the assumption that defect concentration should be very low in comparison to shallow doping concentration, this condition is not always satisfied, particularly in the case of defect-dominated materials [10]. In such cases, nonexponential trap emission often occurs and a careful analysis of the spectra is imperative to extract defect parameters and underlying physics behind the processes leading to unusual features in defect spectra. However, constant-capacitance (CC) DLTS and allied transient techniques have been utilized in the past to overcome the problems related to high trap density [11] and series resistance effect. To overcome the problems related to the temperature scanning method in the conventional

§ Corresponding author.

DLTS technique, various forms of isothermal spectroscopic techniques such as frequency-scanned DLTS [12, 13] and isothermal DLTS [14, 15] have been suggested. However, they have not been as extensively used as conventional DLTS, primarily due to the limitations in scanned frequency range and associated electronics.

This work aims at understanding the unusual features in charge relaxation characteristics from defects in heavily damaged silicon, induced by MeV Ar$^+$ ion implantation. The heavily damaged layer is embedded within the depletion layer of a Schottky diode on silicon and damage-related defects are characterized using DLTS, thermally stimulated capacitance (TSCAP) and time-analysed transient spectroscopy (TATS) [16] in a CC mode of operation. We show that large concentration of defects D1, being a compensating level, controls the quasi-Fermi level in the damaged region and overall band bending in the depletion region through its occupancy. Unusual features in the TSCAP signal and lineshape of TATS spectra is explained by taking into account the dynamic dependence of trap occupancy and quasi-Fermi level. We provide results from numerical simulations by solving kinetic rate equations for a single trap, to understand the occurrence of narrow lineshape in TATS and DLTS signals. Isothermal transient spectroscopy in CC mode is shown to be the most suitable technique for studying such defect-dominated materials.

2. Experimental details

Phosphorous-doped epitaxial n-type silicon (100) wafers of resistivity 2–4 Ω cm on n$^+$ substrate were used for the present study. Vacuum-annealed back ohmic contacts were made by Al deposition on the n$^+$ substrate. These wafers were irradiated from front (polished) side at room temperature with 1.45 MeV Ar$^+$ ions using a 2 MeV Van de Graaff accelerator. The mean projected ion range estimated from Monte Carlo calculations was ~1.23 μm. Ion doses of 5×10^{13} and 1×10^{14} cm^{-2}, which were just below amorphization threshold, were used to create heavy damage without causing amorphization. The beam current was chosen low ($\ll$microampere) to avoid any significant heating of the sample during irradiation. Schottky diodes were formed with evaporated gold dots of diameter 1 mm on irradiated wafers. The diodes receiving only the heat treatment of 70 °C for 30 min for curing the epoxy contacts will be referred to as as-implanted samples. Some mounted devices were oven annealed at relatively low temperature of 160 °C for 30 min. Capacitance measurements were carried out using a Boonton capacitance meter operated at 1 MHz. In TSCAP measurement, the device is cooled under reverse bias and capacitance was measured in the heating cycle with or without zero-bias filling of traps at the lowest temperature. Zero-bias filling at low temperature was performed by removing the bias for several minutes to ensure maximum occupancy of traps. From transient measurements, the spectroscopic signal was constructed using conventional DLTS as well as TATS analysis. TATS [16] is an isothermal spectroscopic technique based on the sweeping rate window in the time domain, which is in contrast to DLTS where the rate window is kept fixed and the temperature is varied. The

TATS technique is similar to those proposed in [12, 14]. The first-order TATS signal S is given by $S(t) = C(t, T) - C(t + \gamma t, T)$, where C represents the capacitance transient at a temperature T and γ is an experimentally selectable constant. $S(t)$ has a maximum at time t_m when plotted against $\ln(t)$ and emission time constant (τ_e) is related to t_m in a manner similar to the DLTS case [16]. The choice of γ and the order of spectroscopy is guided by the required compromise between resolvability and signal-to-noise ratio. TATS being an isothermal spectroscopic technique, it has several advantages over DLTS, especially in the present case where the nature of transients is strongly temperature dependent. Furthermore, lineshape of the TATS spectra is independent of the trap parameters or the range of time and temperature. Using TATS, lineshape analysis is quite straightforward to detect any occurrence of non-Debye trap signature. We have demonstrated the efficacy of TATS in a number of studies involving defects in semi-insulating GaAs [17], DX centre in Al$_x$Ga$_{1-x}$As [18], ion irradiation induced defects in deep buried layer in Si [8, 19, 20] etc. In a typical TATS measurement, transient data are acquired over $4\frac{1}{2}$ orders of magnitude in time at a stabilized temperature. To avoid nonexponentiality of transient due to high trap density, transient measurements were performed in CC mode where voltage transient is monitored keeping the capacitance constant using a feedback circuit [11]. In CC mode, zero-bias filling of the trap was performed by collapsing the feedback using a junction field effect transistor (JFET) for the desired duration. This scheme was essential for transient measurements at higher temperatures where no appreciable change in capacitance occurs with applied reverse bias voltage.

3. Results and discussion

Figure 1 shows a typical DLTS spectrum for a sample irradiated with MeV Ar$^+$ ions at a dose 5×10^{13} cm^{-2} and subjected to low temperature post-implant annealing (at 160 °C for 30 min). For the chosen rate window, two majority carrier trap-related peaks labelled as V$_2$ and D1 are observed in the temperature range 90–310 K. The peak labelled V$_2$ is a well known peak due to divacancy centre V$_2${−/0} having energy level E_c-0.42 eV, with a capture cross-section $\sim 3 \times 10^{-15}$ cm^2, observed in all ion irradiation processes in n-Si [4]. The peak labelled D1 is the most dominant among all other peaks seen for these samples containing heavy damage. A closer look at the D1 peak shows an unusual feature in the DLTS spectral lineshape: the peak is skewed on the right edge (figure 1). To illustrate the unusual lineshape in the D1 peak, we fitted the DLTS spectra of figure 1 for two traps, assuming exponential transient signal from each of them. The trap parameters required for the fitting was independently determined from CC-TATS measurement, which is described later. In the fitting process, trap energy was treated as constant while capture cross-section related prefactor was adjusted to match the exact peak position observed experimentally. The dotted curve in figure 1 corresponds to a fitted DLTS spectrum assuming the observed peak position to be correct. This clearly shows that the experimental DLTS lineshape for peak D1 is very narrow compared with the peak expected from
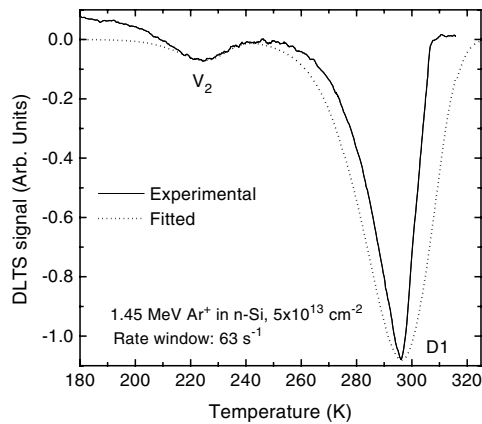
Figure 1. A typical DLTS spectrum of high-dose Ar$^+$-implanted 160 °C annealed n-type Si showing two major trap-related peaks (V$_2$ and D1). Chosen rate window $e_n = 63$ s^{-1}. The dotted curve refers to a fitted DLTS peak obtained by assuming an exponential transient emission. Narrowness in lineshape is clearly seen in the experimentally obtained spectra.

Figure 2. TSCAP signal for as-implanted Si *with* (full curve) and *without* (dotted curve) zero-bias filling of traps. Applied reverse bias 4.5 V. Arrows indicate capacitance step positions corresponding to V$_2$ and D1 levels. Heating rate (β) is 2 K min^{-1}.

an exponential transient. It refers to the that fact that carrier emission from trap D1 follows a nonexponential behaviour.

Figure 2 shows a typical TSCAP spectra for as-implanted Si with and without zero-bias filling of the traps. The sample was cooled under reverse bias with reasonably slow cooling (at a rate ∼4 K min^{-1}). The full curve obtained with zero-biased filling of traps for several minutes at low temperature shows one additional capacitance step at lower temperature (165 K) and a large increase in step height for the other capacitance step at 210 K indicated by arrows. Thus, the TSCAP signal shows the presence of two defect levels. The low-temperature step is due to the divacancy (V$_2$) trap level and the large step at 210 K is due to the damage-related trap D1 shown in figure 1. This defect assignment was verified from the knowledge of the heating rate (β) and the measured temperature (T_m) at which a step occurs in the TSCAP signal and calculated energy level position†. The large step height in the dotted curve (obtained without zero-bias filling) in figure 2 indicates that traps are filled just by lowering the temperature, and with zero-bias filling these traps are additionally filled in larger concentration. This can be understood on the basis of a shift in quasi-Fermi level (E_f) with increasing temperature which in turn causes deoccupation of a large fraction of additional traps at the E_f/E_t crossing point. For example, a temperature change of 200–250 K may cause Fermi-level movement of about 57 meV‡ which is high enough to cause a large change in trap occupancy due to the very sharp trap profile at the edge of the damage profile. Steady state capacitance–voltage measurements on these devices showed that peak concentration of trap density is very high compared with background doping concentration and they are found at a

† The midpoint of the TSCAP step T_m is related to the activation energy E_t by $E_t = kT_m \ln[\gamma k T_m/\beta(E_t + 2kT_m)]$, where β is the heating rate and γ is the attempt to escape frequency for the carrier from the defect. This relation was used to verify the correspondence between E_t and T_m.

‡ In the calculation, a background doping (N_d) of 1×10^{15} cm^{-3} is assumed and the Fermi level is calculated from the relation $E_f = E_i + k_B T \ln(N_d/n_i)$ where $n_i = 3.88 \times 10^{16} T^{3/2} \exp(-7000/T)$ and E_i refers to intrinsic level.
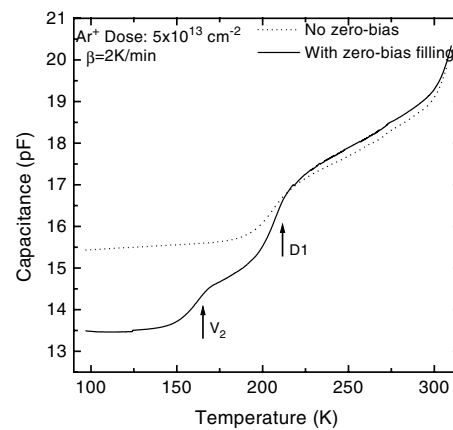
depth much larger than the projected ion range. In as-implanted devices zero-bias depletion width was as large as 3–4 μm in contrast to a width of ∼1.1 μm in the control diode. From model simulation of capacitance–voltage characteristics it has been shown earlier that due to large occupation of the traps, the band becomes almost flat over the distance such defects are present [21]. This trap filling without application of the filling pulse indicates that trap occupancy is controlled by movement of quasi-Fermi level with temperature [22]. From the measured step height in the TSCAP signal, we estimated the trap density using the relation $N_d \cdot \delta W$, where N_d is the shallow dopant concentration and δW is the change in depletion width due to capacitance rise. This amounts to an areal density of 1×10^{11} cm^{-2} which is comparable to background doping concentration in the present samples. From simulation, it was shown that the peak trap concentration can be as high as ten times the background doping concentration in these samples, though only a fraction of these charges are emitted during a transient experiment [21].

The strong temperature dependence of the trap occupancy is exhibited in figure 3 which shows a set of CC-TATS spectra for defect D1 in as-implanted n-Si measured at various temperatures for a fixed depletion width. The depletion width was kept fixed by keeping the capacitance constant through a feedback circuit. In each case, the device was taken to zero bias for 1 s to fill the traps. This filling time duration is large enough to ensure complete filling of the traps as measurement of trap occupancy at 217.6 K showed a saturation in peak height for a filling time of 1.2 s for the D1 trap [19]. As the temperature of measurement is lowered, peak heights are considerably reduced, becoming undetectable at very low temperature. The reduction in peak height could be attributed to the reduced fraction of traps emptied, being smaller at lower temperature. For the set of curves shown in figure 3, due to temperature change alone the Fermi level shifts by several meV and correspondingly an increasing fraction of traps are emptied when the depletion width is kept fixed. A temperature dependence of transient amplitude can give rise to lineshape distortion in a temperature scanning spectroscopic method
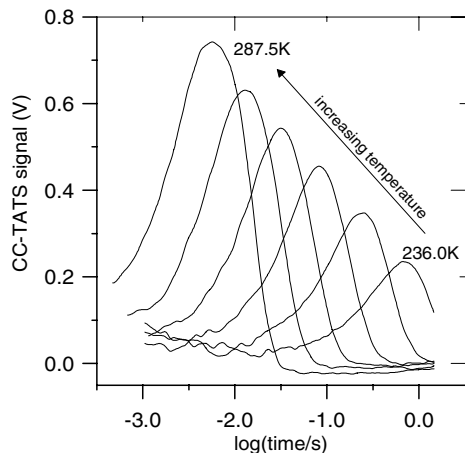
Figure 3. CC-TATS spectra of defect D1 recorded at various temperatures keeping depletion width constant for all temperatures of measurement. In each case the device was driven to zero bias to fill the traps with majority carriers.

such as DLTS. Therefore, a proper analysis could only be made through an isothermal spectroscopic technique such as TATS. The defect D1 is found to be a compensating midgap trap [8] and due to unusual band bending inside the depletion region, these traps are occupied with negative charge giving rise to a large depletion width at lower temperatures. It can be noted that in the CC experiment, as the depletion edge was kept constant for all temperatures shown in figure 3, lowering of temperature causes reduction in quiescent reverse bias voltage across the device. In that case, zero-bias filling pulse samples less volume of the depletion layer which may be partly responsible for the reduced peak height of the CC-TATS signal. The possibility of a thermally activated capture process is not straightforward to verify in this case, since the trapping dynamics were considerably slowed down due to the limited availability of free carrier in the damaged region [19]. Moreover, charge redistribution among multiple traps causes a nonmonotonic change in trap occupancy with filling time [19] and does not allow us to obtain an Arrhenius relationship for determination of the capture barrier. Nevertheless, we believe that the magnitude of the capture cross-section (see table 1) derived from extrapolation of the Arhennius plot is such that a capture barrier is less likely to be present. Our TSCAP measurements using zero-bias filling at low temperature ($\sim$100 K) indicate that a significant fraction of the traps are filled even at such low temperature, indicating no significant capture barrier for this major trap.

A proper inspection of the lineshape for peak D1 shown in figure 3 reveals that peaks are narrower than would be expected due to exponential transient. Figure 4 shows a CC-TATS spectra for 160 °C annealed implanted sample (full curve). The dashed curve (Fit 1) refers to a fitted peak assuming exponential transient with time constant extracted from the apparent (experimental) peak position and the dotted curve (Fit 2) is fitted with an exponential transient considering only the left side of the peak to be real. It was ascertained by a point-by-point analysis [23] of the transient data points that only a single time constant of decay is involved for the left side of the TATS peak. It was found that the apparent peak (position and lineshape) is an

artifact of the premature termination of transient and it is only the later fitting by the dashed curve which is meaningful. Conventional analysis of the experimental spectra, assuming the peak to be real, underestimates the emission time constant as well as trap concentration. Therefore, it is important to use isothermal transient spectroscopy such as TATS in such cases for unambiguous determination of the defect parameters. The true trap parameter obtained by such fitting show that defect D1 is a midgap trap whose energy level lies in the range 0.49–0.56 eV depending on the implantation dose and annealing condition, as given in table 1. The capture cross-section for this defect was estimated to be $\sim$10^{-15} cm^2. At lower temperatures of measurement, broadening of lineshape is observed related to damage-related lattice strain, which gives rise to a broadening in energy level. The change in broadening with dose is shown in table 1. Energy broadening in the high-dose implanted sample is found to be significant (25 meV) and it can be used to probe the degree of strain related to disorder in heavily damaged material. The change in broadening due to low-temperature processing is not significant. The occurrence of sudden cessation of the emission transient leading to skewed peak in DLTS or TATS can be understood in terms of dynamics of quasi-Fermi level movement and trap occupation. During the transient experiment, on restoration of reverse bias immediately after filling pulse, the depletion width increases considerably owing to large increase in negative charge in the damaged layer, thus pushing the Fermi level down below the trap level in the damaged region. This leads to exponential emission of carrier from extra trapped charge until the quasi-Fermi level hits the trap level, quickly bringing emission transient to an end. This process is crucially dependent on the fact that the emitting centre itself controls the quasi-Fermi level in the damaged region and the overall band bending through its occupancy. It is worth mentioning here that in standard cases of small trap concentration, band bending is primarily controlled by the background shallow dopants. For the present case, trap concentration is so large that it controls the band bending in the region of its presence, which in turn determines the crossing point between trap energy level and Fermi level. The spatial location of the crossing is determined by the dynamics of the defect occupation.

In a previous report we have shown that these defects migrate to a very large depth compared with their expected profile derived from standard Monte Carlo simulations. From the migrating nature of these defects it was concluded that they are interstitial cluster related [21]. Studies on thermal stability of the dominant defect D1 provided evidence that D1 originates from interstitial cluster defects of relatively small size [24, 25]. Reports on DLTS studies of the energy level for interstitial defect clusters show that multiple energy levels are introduced in the band gap of silicon, depending on the implantation fluence and post-implant annealing conditions in both n- and p-type silicon, though they were found to be more prominent in p-type silicon [25]. We found one major defect in as-implanted n-Si which introduces a midgap level in the band gap and similar levels have been observed in the literature [25].

The interdependence of quasi-Fermi level and trap occupancy is further demonstrated from the temperature

Table 1. Variation of trap (D1) parameter (energy level ($E_C - E_T$), Gaussian broadening in energy level (ΔE_T), capture cross-section (σ_n)), with implantation dose and low-temperature annealing conditions.

Ar$^+$ ion dose (cm^{-2})	As-implanted			160 °C annealed		
	$E_C - E_T$ (eV)	ΔE_T (eV)	σ_n (cm^2)	$E_C - E_T$ (eV)	ΔE_T (eV)	σ_n (cm^2)
5×10^{13}	0.54	0.006	2.4×10^{-15}	0.56	0.006	7.4×10^{-16}
1×10^{14}	0.49	0.025	7.7×10^{-16}	0.52	0.025	1.1×10^{-15}
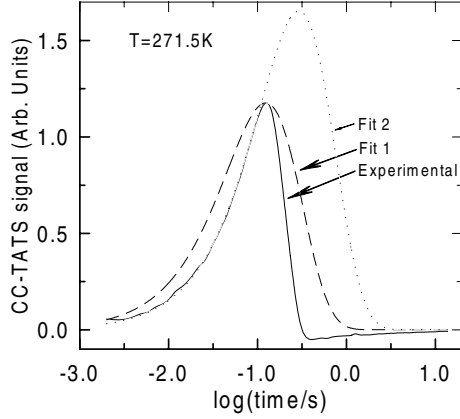
Figure 4. CC-TATS spectra (full curve) for Ar$^+$-implanted 160 °C annealed n-Si sample. The dashed curve (Fit 1) refers to peak fitting assuming an exponential transient with time constant derived from the apparent peak position. The dotted curve (Fit 2) is fitted with an exponential transient considering only the left side of the peak to be proper.
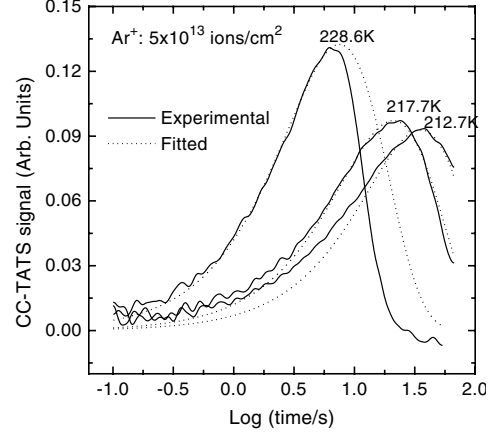
Figure 5. CC-TATS spectra (full curves) of defect D1 measured at temperatures 212.7, 217.7 and 228.6 K. The dotted curve in each case corresponds to peak fitted with exponential transients showing a broad, exponential and narrow peak, respectively, with increasing temperature.

dependence of lineshape in CC-TATS spectra presented in figure 5. The full curves refer to experimental spectra recorded at three different temperatures and the dotted curves refer to the fitting assuming an exponential transient with time constant derived from peak position. While at higher temperature ($T = 228.6$ K) the peak is narrower than that expected due to exponential transient, peaks show broadening when measured at lower temperatures ($T = 212.7$ K). The dynamic effect is reduced at lower temperatures of measurement and there is a correspondingly reduced effect of quasi-Fermi level movement giving rise to the usual peakshape expected from a slightly broadened energy level. The broadness in peaks is expected due to lattice strain surrounding these defects in the damaged layer [26]. A distribution in size of the cluster-type defects and surrounding strain at the defect site would give rise to such broadened energy levels (see table 1).

In the literature, occurrence of broad spectral lineshape has been explained by assuming a broad density of states which may result from lattice strain, disorder, alloy fluctuation etc in different situations. However, no mechanism has been visualized yet in the literature to explain the occurrence of narrow lineshape in DLTS or TATS spectra. It is easily understandable that a specific kind of nonexponential emission may give rise to such narrow lineshape in spectra. In an attempt to understand more details of the dynamics giving rise to unusual lineshape in the spectra, we consider here a model assuming a single trap in the energy gap. The rate equation controlling the trapping and detrapping dynamics of the trap (density N_T) in n-type

material can be expressed as

$$\frac{dn_t}{dt} = -e_n n_t + c_n n(N_T - n_t), \qquad (1)$$

where n_t is the density of occupied trap, e_n is the emission rate, c_n is the capture constant, n is the free-carrier density and N_T is the total trap density. During trap emission under reverse bias, the capture term (second term) in equation (1) is negligible and the solution for $n_t(t)$ yields an exponentially decaying transient. However, when the free-carrier concentration is time dependent due to its being controlled by trap occupancy, the capture term is non-negligible. To model the dynamics of quasi-Fermi level movement upwards during trap emission, we introduce here an exponentially varying free-carrier density (n) of the form

$$n(t) = n_0[1 - A \exp(-e_n t)]. \qquad (2)$$

We normalize equation (1) with respect to N_T for ease of calculation without requiring an absolute concentration of trap. Assuming model parameters for e_n, c_n and A, equations (1) and (2) are solved numerically to obtain the time dependence of n_t and we show a TATS spectra in figure 6 corresponding to the simulated transient. The full curve refers to simulated spectra obtained from equations (1) and (2), while the dashed curve (Fit 1) refers to a fitted peak assuming an exponential transient, which clearly shows the narrowness in lineshape of the simulated spectra. The dotted curve (Fit 2) shows a peak fitted assuming an exponential
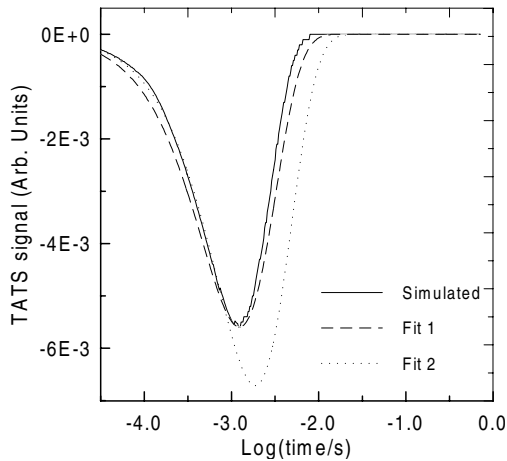
Figure 6. Simulated TATS spectra (solid curve) assuming a time-dependent capture term in the dynamic rate equations governing the occupancy of the major trap. The dashed curve (Fit 1) refers to a peak fitted with exponential transient and the dotted curve (Fit 2) refers to a peak fitted with an exponential transient assuming only the left side of the peak to be undistorted. The parameters used for solving equation (1) are $e_n = 9.6 \times 10^2$ s^{-1}, $c_n n_0 = 20$ s^{-1} and $A = 0.5$.
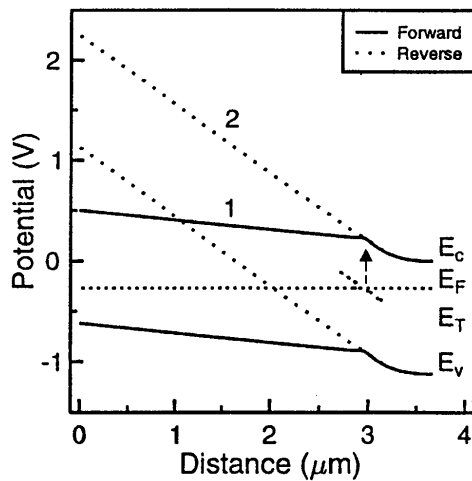
Figure 7. Energy band diagram for a Schottky diode on n-type Si under (1) forward bias (all traps occupied) and (2) reverse bias (traps partially de-occupied) showing the unusual band bending, dynamics of trap emission and quasi-Fermi level movement. The dashed arrow indicates upward movement of E_f during trap emission resulting in a premature termination of transient when E_f crosses E_t and an increase in λ-region width.

transient such that the left side of the peak fits well. This clearly shows that the simulated peakshape is unusual due to the presence of a time-dependent capture term in equation (1) and that a nonexponential transient of this kind can give rise to narrow lineshape in spectra. Note that these features in figure 6 closely resemble those of the experimental data shown in figure 4. As argued earlier, premature termination of the emission transient can be understood in terms of dynamic change in quasi-Fermi level and trap occupancy, which causes carrier capture to be significant at a later stage of emission, and this is taken into account in equation (2) through an exponentially rising $n(t)$. Therefore, our simulation provides strong support for the model presented above to explain the

unusual features in spectral lineshape. The essential features of this model can be represented by an energy band diagram as shown in figure 7, where E_c, E_v, E_t and E_f refer to the conduction band edge, valence band edge, activation energy of the trap and Fermi level, respectively. Under zero- or forward-bias condition of device, the traps are occupied by negative charge, causing flattening of the band in the depletion region due to the high density of traps. To obtain the band bending in the depletion region, a one-dimensional Poisson equation was solved numerically for a Gaussian distribution of trap profile and details of the procedure can be found elsewhere [21]. To account for the large depletion width, it was necessary to have a compensated region in the depletion region and a high density of traps near the edge of the depletion region. At the end of the trap-filling pulse, under reverse bias the traps above the Fermi level are emptied and band bending changes correspondingly. As these trap levels are compensating centres, free-carrier density increases with carrier emission from traps and correspondingly the quasi-Fermi level moves upwards (shown with a dashed arrow). This causes the rest of the trap levels (near the E_t/E_f crossing point inside the depletion region) to come below the quasi-Fermi level and, consequently, carrier emission stops prematurely, before the time it would have taken in the absence of quasi-Fermi level movement. Although the details of the band bending in the depletion region is decided by the exact trap profile, the traps at the E_t/E_f crossing point are affected most by this dynamic process and this gives rise to the unusual features in spectral lineshape. Such dynamics is to be expected in the case of a high density of compensating traps localized in a small region in the device.

4. Conclusions

The electrical manifestation of damage and defects distinct to the regime of heavy damage induced by high-dose MeV Ar$^+$ implantation have been investigated in n-type silicon using transient capacitance techniques. DLTS and TSCAP studies on as-implanted Si samples showed the presence of the divacancy trap and a damage-related trap (D1) in large concentration. The trap D1 is shown to control the quasi-Fermi level in the damaged region through its occupancy which strongly depends on temperature. Dynamic interdependence of trap occupancy and quasi-Fermi level is believed to cause premature termination of capacitance/voltage transient during trap emission. The essential features of the spectral lineshape is simulated by introducing a time-dependent capture term in the rate equation for the major trap and this supports our model on the dynamic interdependence of trap occupancy and quasi-Fermi level. The trap parameters are found to be sensitive to the implantation dose and low-temperature processing conditions. This major trap is speculated to be small interstitial cluster related. The critical role of isothermal spectroscopy and the CC mode of measurement are demonstrated for the study of defect-dominated materials such as in the present case.

Acknowledgments

References

[1] Borland J O and Koelsch R 1993 *Solid State Technol.* **36** 28
[2] Chason E *et al* 1997 *J. Appl. Phys.* **81** 6513
[3] Wang K L 1980 *Appl. Phys. Lett.* **36** 48
[4] Svensson B G, Mahajderi B, Hallen A, Svensson J H and
    Corbett J W 1991 *Phys. Rev.* B **43** 2292
    Svensson B G, Jagadish C, Hallen A and Lalita J 1997 *Phys.
    Rev.* B **55** 10 498
[5] Zaraiz M, Gilmer G H, Poate J M and De le Rubia T D 1996
    Appl. Phys. Lett. **68** 409
[6] Benton J L, Libertino S, Kringhoj P, Eaglesham D J,
    Poate J M and Coffa S 1997 *J. Appl. Phys.* **82** 120
[7] Hardalov Ch M, Stefanov K D and Sueva D 1995 *Appl. Phys.*
    A **61** 107
[8] Giri P K and Mohapatra Y N 1997 *Appl. Phys. Lett.* **71** 1682
[9] Lang D V 1974 *J. Appl. Phys.* **45** 3023
[10] Mohapatra Y N, Agarwal S and Giri P K 1998 *Physics of
    Semiconductor Devices* ed V Kumar and S K Agarwal
    (New Delhi: Narosa) p 1109
[11] Johnson N M, Bartelink D J, Gold R B and Gibbons J F 1979
    J. Appl. Phys. **50** 4828
[12] Henry P M, Meese J M, Farmer J W and Lamp C D 1985 *J.
    Appl. Phys.* **57** 628
[13] Ferenczi G, Boda J and Pavelka T 1986 *Phys. Status Solidi* a
    94 K119
[14] Turchanikov V I, Lysenko V S and Gusev V A 1986 *Phys.
    Status Solidi* a **95** 283
[15] Okusi H and Takumaru Y 1990 *Japan. J. Appl. Phys.* **19** L335
[16] Agarwal S, Mohapatra Y N and Singh V A 1995 *J. Appl.
    Phys.* **77** 3155
[17] Giri P K and Mohapatra Y N 1995 *J. Appl. Phys.* **78** 262
[18] Agarwal S, Mohapatra Y N, Singh V A and Sharan R 1995 *J.
    Appl. Phys.* **77** 5725
[19] Giri P K, Dhar S, Kulkarni V N and Mohapatra Y N 1998
    Phys. Rev. B **57** 14 603
[20] Giri P K and Mohapatra Y N 2000 *Phys. Rev.* B **62** 2496
[21] Giri P K and Mohapatra Y N 1998 *J. Appl. Phys.* **84** 1901
[22] Zhaohuai Liu J and Wagner S 1989 *Phys. Rev.* B **39** 11 156
[23] Mangelsdorf P C Jr 1959 *J. Appl. Phys.* **30** 442
[24] Giri P K and Mohapatra Y N 2000 *Mater. Sci. Eng.* B **71** 327
[25] Benton J L, Halliburton K, Libertino S, Eaglesham D J and
    Coffa S 1998 *J. Appl. Phys.* **84** 4749
[26] Omling P, Weber E R, Montelius L, Alexander H and
    Michel J 1985 *Phys. Rev.* B **32** 6571